Published in "Genetics 188(1): 91-103, 2011"
which should be cited to refer to this work.

Heat Avoidance Is Regulated by Transient Receptor Potential (TRP) Channels and a Neuropeptide Signaling Pathway in *Caenorhabditis elegans*

Dominique A. Glauser,*,[1] Will C. Chen,† Rebecca Agin,* Bronwyn L. MacInnis,*,[2] Andrew B. Hellman,‡ Paul A. Garrity,§ Man-Wah Tan,†, and Miriam B. Goodman*,[3]**

*Departments of *Molecular and Cellular Physiology †Genetics, ‡Biology, and **Microbiology and Immunology, Stanford University, Stanford, California 94305 and §Department of Biology and Center for Behavioral Genomics, Brandeis University, Waltham, Massachusetts 02454*

ABSTRACT

The ability to avoid noxious extremes of hot and cold is critical for survival and depends on thermal nociception. The TRPV subset of transient receptor potential (TRP) channels is heat activated and proposed to be responsible for heat detection in vertebrates and fruit flies. To gain insight into the genetic and neural basis of thermal nociception, we developed assays that quantify noxious heat avoidance in the nematode *Caenorhabditis elegans* and used them to investigate the genetic basis of this behavior. First, we screened mutants for 18 TRP channel genes (including all TRPV orthologs) and found only minor defects in heat avoidance in single and selected double and triple mutants, indicating that other genes are involved. Next, we compared two wild isolates of *C. elegans* that diverge in their threshold for heat avoidance and linked this phenotypic variation to a polymorphism in the neuropeptide receptor gene *npr-1*. Further analysis revealed that loss of either the NPR-1 receptor or its ligand, FLP-21, increases the threshold for heat avoidance. Cell-specific rescue of *npr-1* implicates the interneuron RMG in the circuit regulating heat avoidance. This neuropeptide signaling pathway operates independently of the TRPV genes, *osm-9* and *ocr-2*, since mutants lacking *npr-1* and both TRPV channels had more severe defects in heat avoidance than mutants lacking only *npr-1* or both *osm-9* and *ocr-2*. Our results show that TRPV channels and the FLP-21/NPR-1 neuropeptide signaling pathway determine the threshold for heat avoidance in *C. elegans*.

TEMPERATURE influences each and every biological and biochemical process. Thus, the ability to sense temperature and respond adequately is critical for the survival of all organisms. In both endotherms and ectotherms, behavioral responses to environmental temperature are essential to maintain body temperature in a range that is suitable for growth and reproduction (Hafez 1964; Gentry 1973; Huey 1974; Seebacher 1999). Additionally, the sensation of noxious temperature, also called thermal nociception, induces adaptive avoidance behaviors that minimize the risk of tissue damage.

The range of temperatures that sustain growth and those that produce damage vary widely among animal species. Innate behavioral responses to temperature have probably evolved to match specific habitats and physiology. For example, the threshold for activation of the cold-sensitive ion channel TRPM8 correlates with core body temperature in vertebrates (Myers *et al.* 2009). Genetic variations also modulate nociception and temperature sensation within species. In humans, examples include genetic diseases, such as the congenital insensitivity to pain with anhydrosis (Indo 2001) and three pain disorders caused by nonsense and gain-of-function mutations in the SCN9A channel gene (Drenth and Waxman 2007). Polymorphisms in several genes appear to associate with variations in thermosensation and nociception, including TRPA1 (Kremeyer *et al.* 2010), SCN9A (Drenth and Waxman 2007; Reimann *et al.* 2010), and catechol-*O*-methyltransferase (Diatchenko *et al.* 2005). Such intraspecific variations provide valuable insights to understand the genetic, molecular, and cellular basis of temperature sensation and nociception as well as the downstream mechanisms leading to physiological and behavioral responses. Because key experiments necessary to advance our understanding of those mechanisms are impossible in humans and hindered by the complexity of the nervous system in mammalian models, the use of simpler model organisms is beneficial.

Caenorhabditis elegans is a small nonparasitic nematode that grows and reproduces <27°; reproduction is optimal near 20° (Felix and Braendle 2010). In the

[1]*Present address:* Department of Biology/Zoology, University of Fribourg, 1700 Fribourg, Switzerland.

[2]*Present address:* Wellcome Trust Sanger Institute, Hinxton CB10 1SA, United Kingdom.

[3]*Corresponding author: Department of Molecular and Cellular Physiology, Stanford University,* B-111 Beckman Center, 279 Campus Dr., Stanford, CA 94305. E-mail: mbgoodman@stanford.edu

laboratory, *C. elegans* uses thermotaxis and isothermal tracking to locate favorable regions in thermal gradients <27°. They show some plasticity regarding their preferred temperature, which depends on feeding status and previous cultivation temperature (Hedgecock and Russell 1975; Chi *et al.* 2007). Studies on thermotaxis led to the identification of a pair of thermoreceptor neurons, called AFD, as well as several genes required for the temperature-related behaviors (reviewed by Garrity *et al.* 2010). In addition to thermotaxis, *C. elegans* has been reported to produce a stereotyped avoidance response when encountering high temperature regions (Wittenburg and Baumeister 1999). The threshold for this thermal avoidance response is not known. The molecular and neuronal basis for this behavior is also largely unexplored (Garrity *et al.* 2010).

The classical laboratory strain of *C. elegans* is the Bristol isolate, N2. Many isolates have been recovered from around the world and can be grown in the laboratory. Recent studies have used this panel of wild isolates to address questions related to the genetic variability within *C. elegans* (Sivasundar and Hey 2003; Cutter 2006; Rockman and Kruglyak 2009). A high density of single nucleotide polymorphisms (SNPs) between the Hawaiian isolate CB4856 and N2 enables the use of CB4856 for mapping mutations generated in the N2 background (Wicks *et al.* 2001; Davis *et al.* 2005). In addition, quantitative trait loci (QTL) approaches and near isogenic lines (NIL), made from introgression of CB4856 into the N2 background, have been used to investigate the genetic basis of phenotypic variations across the two strains (Kammenga *et al.* 2008; Doroszuk *et al.* 2009; McGrath *et al.* 2009). Of note, thermotaxis behavior in CB4856 is quite different from that in N2 (Anderson *et al.* 2007). Nothing is known, however, regarding differences in sensitivity to noxious heat between N2 and CB4856.

In this study, we used genetic dissection of mutant and polymorphic *C. elegans* strains to show that heat avoidance is mediated by two parallel pathways: one that is TRPV dependent and a second that relies on neuropeptide signaling that is polymorphic among wild *C. elegans* isolates. We developed two new behavioral assays to quantify *C. elegans* thermonociception and used these assays to screen for behavioral defects in animals with mutations in 18 TRP channel genes and for variations between the Bristol and Hawaiian *C. elegans* strains. Except for the TRPV channel mutant *osm-9*, which displayed a mild defect in thermal nociception, TRP channel single mutants retained the ability to avoid noxious heat. The threshold for noxious heat avoidance was higher in the Hawaiian *C. elegans* strain. We showed that this behavioral difference is linked to polymorphisms in the *npr-1* neuropeptide receptor gene. Loss-of-function mutations in *npr-1* and the peptide ligand-encoding gene *flp-21* in the Bristol background phenocopy the behavior of the Hawaiian strain. Furthermore, rescue experiments and epistasis analyses indicate that wild-type *npr-1* is likely to act in the RMG interneuron and that this neuropeptide signaling pathway acts in parallel with the TRPV-dependent pathway. Taken as a whole, our results show that the thermal threshold for heat avoidance is genetically tuned in *C. elegans* and suggest that both NPR-1–dependent and TRPV-dependent signaling pathways regulate the heat avoidance behavior.

MATERIALS AND METHODS

Phylogeny of TRP channel genes: Multiple sequence alignment (MSA) was performed using ProbCons (Do *et al.* 2005) for the region extending from the two transmembrane (TM) domains N terminal to the pore loop through the TM domain immediately C terminal to the pore loop; *e.g.*, TM4–TM6 for TRPA channels. Prior to maximum likelihood analysis, gaps in the MSA were minimized by manual editing to remove regions of nonalignment. Maximum likelihood analysis was performed with PhyML 3.0 (Guindon *et al.* 2009), using LG substitution rate matrix (Le and Gascuel 2008) and gamma-distributed rate variation (four categories), and bootstrapped 100 times.

Worm maintenance and strains: Worms were maintained on *Escherichia coli* OP50 bacteria according to standard cultivation protocols (Brenner 1974). *C. elegans* strains used in this work were: N2, CB4856, TR403, AB3, LW1288 *arIs37* I; *sma-6(jj1)* II; *cup-5(ar465)* III, RB1052 *trpa-1(ok999)* IV, RB2351 *trpa-2 (ok3189)* I, VC160 *trp-1(ok323)* III, VC602 *trp-2(gk298)* III, VC818 *trp-4(gk341)* I, EJ26 *gon-2(q362)* I, VC244 *gtl-1(ok375)* IV, RB1787 *F56F11.5(ok2305)* III, RB1883 *W03B1.2(ok2433)* IV, RB1478 *F13B12.3(ok1729)* IV, PT8 *pkd-2(sy606)* IV; *him-5 (e1490)* V, RB753 *lov-1(ok522)* II, CX10 *osm-9(ky10)* IV, CX4533 *ocr-1(ok132)* V, CX4544 *ocr-2(ak47)* IV, RB1374 *ocr-3 (ok1559)* X, LX950 *ocr-4(vs137)* IV, LX845 *ocr-2(ak47)* IV; *ocr-1 (ok132)* V, LX980 *ocr-4(vs137)* IV; *ocr-1(ok132)* V, LX981 *ocr-4 (vs137) ocr-2(ak47)* IV, LX748 *osm-9(ky10) ocr-2(ak47)* IV, FG125 *osm-9(ky10) ocr-2(ak47)* IV; *ocr-1(ak46)* V, DA609 *npr-1(ad609)* X, CX4148 *npr-1(ky13)* X, DA508 *npr-1(n1353)* X, RB982 *flp-21 (ok889)* V, GN376 *flp-21(ok889)* V; *npr-1(ad609)* X, GN377 *osm-9(ky10) ocr-2(ak47)* IV; *npr-1(ad609)* X, QX1155 *qqIR1*(X, CB4856 N2) X, CX10860 *qqIR1*(X,CB4856 N2) X; *kyEx2800 [Pnpr-1::npr-1(215V):sl2gfp Pelt-2::mCherry]*, CX11038 *qqIR1*(X, CB4856 N2) X; *kyEx2892 [Pnpr-1::npr-1(215F):sl2gfp Pelt-2:: mCherry]*, CX7102 *qaIs2241 [Pgcy-35::GFP Pgcy-36::egl-1 lin15+]* X, CB1611 *mec-4 (e1611)* X, CX9592 *npr-1(ad609)* X; *kyEx2061 [npr-1::npr-1 SL2 GFP, ofm-1::dsRed]*, CX9395 *npr-1(ad609)* X; *kyEx1965 [gcy-32::npr-1 SL2 GFP, ofm-1::dsRed]*, CX9633 *npr-1 (ad609)* X; *kyEx2096 [flp-8::npr-1 SL2 GFP, ofm-1::dsRed]*, and CX9396 *npr-1(ad609)* X; *kyEx1966 [flp-21::npr-1 SL2 GFP, ofm-1::dsRed]*. The chromosome substitution strains, CSSI, CSSII, CSSIII, CSSIV, CSSV, and CSSX, will be described in detail elsewhere (W. C. Chen and M.-W. Tan, unpublished results). The generation of the CSSXB strain (strain name GN360) and the AFD ablated strain (GN112) is described below.

Plate preparation for behavioral assays: The agar medium used for behavior assays was identical to nematode growth media (NGM), except that cholesterol and bactopeptone were omitted. After autoclaving, medium (10 ml) was poured into rectangular Petri dishes (7.6 cm $l \times 5$ cm $w \times 1$ cm d, Lab Scientific, Livingston, NJ). These plates contain a small well (6 mm diameter) located in the middle of one of the long

edges (which was used in the *thermal barrier assay*). Plates were prepared the same day as the assays were performed and left open at room temperature for cooling and drying until they had lost ~20% of their initial weight due to evaporation, a process which was completed in 1–2 hr, depending on room temperature and humidity.

Chemical attractant cocktail: Isoamyl alcohol (1:200) and 2,3-butanedione (1:20,000) were diluted in ethanol. To achieve a 1:20,000 dilution, 2,3-butanedione was first diluted to 1:100. The final attractant cocktail and the intermediate dilutions were made fresh daily.

Worm starvation: Worms were collected with MilliQ purified water in 1.5-ml microcentrifuge tubes, centrifuged for 3 sec on a low-speed benchtop mini centrifuge, and washed twice. A dense worm pellet was transferred and gently brushed onto bacteria-free NGM dishes. Plates were sealed with Parafilm and kept at 20° for 5–6 hr prior to assays. This procedure was sufficient to eliminate food-dependent thermotaxis (Chi *et al.* 2007; Ramot *et al.* 2008).

Thermal barrier assay: Assay plates were placed on an aluminum plate, whose temperature was held constant by thermoelectric coolers, as described (Ramot *et al.* 2008). Controllers were set such that the temperature measured away from the barrier at the top of the agar surface was 21°. A thermal barrier was generated by flowing heated water through an aluminum tube (length, 10 cm; inner diameter, 0.9 mm; outer diameter, 1.6 mm) maintained at a constant distance over the agar surface (see below). Water temperature was controlled by a circulating bath (Lauda B, Königshoffen, Germany) and could be varied to generate defined thermal barrier temperature. The rectangular plates for the thermal barrier assay were modified by the creation of two slits allowing the heated metal tube to move freely on the vertical axis. The distance between the metal tube and the agar surface was set by three spacers made of polyethylene tubing of 0.61 mm in external diameter (PE-10; B-D Intramedic, Franklin Lakes, NJ). Temperature of the agar surface below the thermal barrier was measured with a small thermistor (0.5 mm $d \times 2.2$ mm l, TS91-196; McShane, Medina, OH).

Prior to each assay, starved animals were collected in water, centrifuged, and transferred in suspension (10 μl) to the left side of the assay plate (Figure 1A). This aliquot of worms (containing 200–400 worms) was gently brushed over the starting area to allow animals to disperse. Excess liquid was allowed to absorb into the plate and/or evaporate for ~1 min. During this time, the attractant cocktail (10 μl) was added into the built-in well on the right side of the assay plate. The right side of the plate, up to the barrier, was covered with a lid and worms were left to crawl for 10 min. The assay was stopped by exposing worms to chloroform vapor as described (Ramot *et al.* 2008) and worms on each side of the barrier were counted under a stereomicroscope. Scores are presented as the fraction of worms avoiding the barrier.

Noxious heat thermogradient assay: The worm transfer method and temperature-control setup were the same as for the barrier assay. Plates were positioned such that their short sides were parallel to isotherms and temperatures were adjusted to produce a linear thermal gradient centered at 32.8°. On average, the gradient steepness was 1.15°/cm. The attractant cocktail was added to a small well made from the inverted cap of a PCR tube (250 μl) and positioned opposite the starting area (Figure 2A). Animals crawled in this thermochemical environment for 15 min with the lid closed. Surface temperatures increased during the first 3 min after lid closure, but were stable thereafter. At the end of the assay, the lid was removed and the temperature in the center of the plate was measured with an infrared thermometer (Dual Temp Plus; Mastercool, Randolph, NJ), followed by imaging with a CCD camera (DMK 21BU04; The Imaging Source, Charlotte, NC) illuminated obliquely with a custom-built ring of red light-emitting diodes (LEDs).

The distribution of worms was determined from digital images as follows. The position of each worm was determined by its centroid using particle tracking macros in ImageJ, the plate was divided into 15 bins of equal size along the long side (42.6 pixels corresponding to 4.7 mm), and the number of worms in each bin was determined automatically. Each image (640 × 480 pixels) was preprocessed using background subtraction and manual threshold adjustment. The fraction >33° was calculated from these distributions. The end-point temperature measurement in the center of each assay plate was used to correct each distribution profile for minor assay-to-assay variations in temperature, which were <0.2° (32.8° ± 0.2°, mean ± SD, $n = 646$). To assess differences regarding motility and attraction to odorants among strains, control assays were run in absence of the heat gradient at two constant temperatures (21° and 31°; supporting information, Figure S1).

Thermotaxis assay: Well-fed animals were tested in thermotaxis assays as previously described (Ramot *et al.* 2008). We ensured homogenous developmental and feeding states across cultivation plates by adjusting animal density such that food was constantly available during their development. Animals were transferred to new OP50 seeded plates 3–4 hr prior to behavioral assays.

SNP mapping: CB4856 hermaphrodites were mated with N2 males. Several hundred F_2 hermaphrodites were propagated on 15-cm plates for at least three generations of self-fertilization. Eighty-eight animals were used to establish recombinant lines and their F_2 progeny tested using the *noxious heat thermogradient assay*. We classified clones on the basis of the fraction of animals >33°: (i) low score clones unambiguously behaving like N2 (12 clones) and (ii) high score clones unambiguously behaving like CB4856 (14 clones). The remaining 62 clones were not analyzed.

SNP mapping analysis was performed with a previously described set of markers (Davis *et al.* 2005). For each marker, the logarithm of odds ratio (LOD) score was calculated to report genotype/phenotype association. LOD scores reported are the sum of LOD scores obtained by dividing the frequencies of N2 and CB4856 alleles within the low score group and of the LOD scores obtained by dividing the frequencies of CB4856 and N2 alleles within the high score group.

Generation of the CSSXB chromosome substitution strain: HA1134 hermaphrodites (an integrated line carrying the *rtIs27* Posm-10::GFP transgene on the right arm of chromosome X in N2 background) were outcrossed five times with CB4856 males. At each outcrossing, we selected animals carrying the GFP marker as well as the N2 version of a SNP at position −8.14 cM on chromosome X. After the last outcrossing, 30 clones were screened to establish a strain in which the X chromosome was derived almost entirely from the N2 parental strain. Previously described SNP markers were used to validate this strain (Davis *et al.* 2005), which we named CSSXB; the complete SNP profile of CSSXB (also known as GN360) is presented in Table S1. We were not able to fully replace the N2 genome on the left arm of chromosome I, presumably due to the effect of the *zeel-1 peel-1*–mediated genetic incompatibility (Seidel *et al.* 2008). Markers tested on chromosomes II, III, IV, and V, as well as on parts of chromosome I, were all CB4856 variants, but we cannot rule out that some DNA segments from N2 origin have been retained between SNP markers by multiple recombination events.

Genetic ablation of AFD: AFD was killed by driving reconstructed caspase expression under the control of the AFD-specific *gcy-8* promoter. The cDNA sequences of two caspase

subunits (Chelur and Chalfie 2007) were inserted into pSM vectors (Klassen and Shen 2007) between *Bam*HI and *Eco*RI sites. The *gcy-8* promoter was then inserted upstream between *Sph*I and *Bam*HI sites. These vectors were injected into worms jointly with a vector driving expression of mCherry under the control of the *gcy-8* promoter and a vector driving GFP under the control of the *unc-122* promoter, which labels coelomocytes (Loria *et al.* 2004). Animals expressing GFP in coelomocytes, but lacking neuronal mCherry labeling (which indicates loss of AFD) were crossed with worms harboring transgenes expressing GFP in AFD (under the control of the *gcy-8* promoter) and AIY (under the control of the *ttx-3* promoter), so that the loss of AFD and retention of wild-type AIY could be detected. Animals expressing GFP in coelomocytes and AIY, but lacking GFP expression in AFD were selected and an integrated line was made after irradiation with gamma rays. This strain was backcrossed into N2 once and named GN112 (*pgIs1*).

Reagents: Chemicals were obtained from Sigma (St. Louis, MO), PCR master mix from Qiagen (Valencia, CA), and restriction enzymes from New England Biolabs (Ipswich, MA).

RESULTS

Two new assays quantify heat avoidance behavior in *C. elegans*: Until now, heat avoidance in *C. elegans* has been characterized by using assays that stimulate individual animals with a heated metal probe or infrared laser pulses (Wittenburg and Baumeister 1999; Stephens *et al.* 2008). However, such approaches are low throughput and associated with difficulties in measuring the size of the delivered thermal stimulus. To facilitate genetic analyses of heat avoidance, we developed two new quantitative behavioral assays, both of which record the distribution of animal populations on a solid agar surface as a function of defined heat application.

In the thermal barrier assay (Figure 1), worms are placed on one side of an assay plate and migrate to the other side, motivated by an attractive chemical odorant cocktail. Worms must cross under a thermal barrier, created by suspending a heated aluminum tube above the agar surface. Because the barrier is high enough to allow animals to crawl freely underneath, it introduces no physical obstacles. While the odorant cocktail is not required to observe heat avoidance, it drives animals toward the barrier, increasing the resolution of the assay and decreasing the time required to complete each trial.

In this assay, animals are challenged with a sharp increase in temperature as they crawl under the barrier (Figure 1B). Because it is not possible to create an infinitely sharp heat boundary, however, animals moving toward the barrier first encounter warm temperatures likely to engage the thermotaxis behaviors that operate <27°. To minimize the contribution of such behaviors, we used animals deprived of food for >5 hr, since this manipulation abolishes thermotaxis (Chi *et al.* 2007; Ramot *et al.* 2008). Under these conditions, worms responded to the barrier with stereotyped avoidance responses (File S1) similar to those reported previously in well-fed animals and in the absence of an odorant cocktail (Wittenburg and Baumeister 1999; Stephens *et al.* 2008).

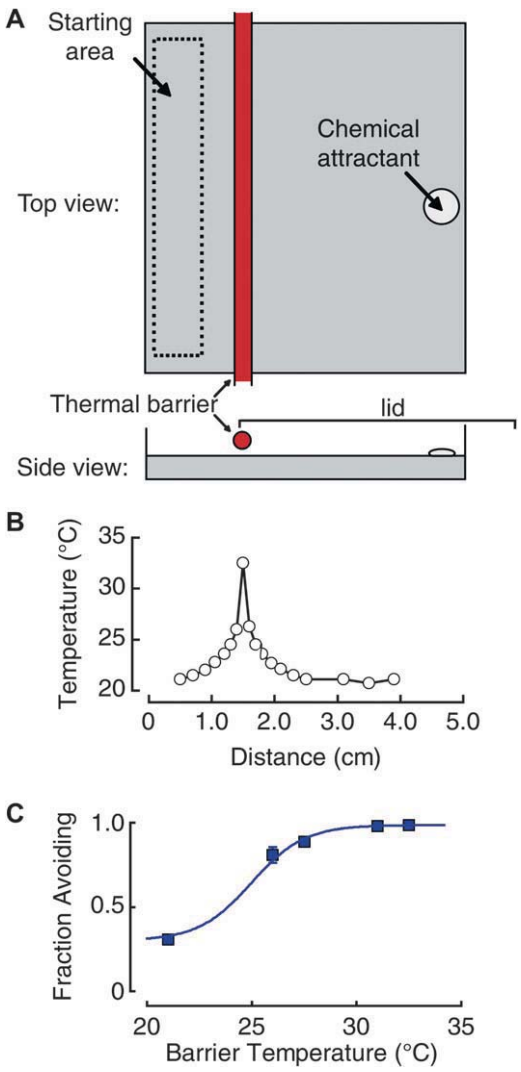

Figure 1.—The *thermal barrier assay.* (A) Schematic of the thermal barrier assay. Two hundred to 400 animals are placed in the starting area opposite a cocktail of chemical attractants (isoamyl alcohol and 2,3-butanedione). A sharp thermal barrier is established by suspending a heated metal tube high enough over the agar surface for worms to crawl freely underneath. A lid closes the attractant side of the plate. (B) Temperature as a function of distance along the agar surface. (C) Fraction of N2 worms avoiding the barrier as a function of its temperature. $T = 21°$ is the control situation in which the metal tube is not heated. Results are means of at least three independent assays; error bars are SEM and are smaller than data points in some cases.

To measure the threshold for thermal avoidance, we varied the barrier temperature and scored the response by counting the fraction of worms avoiding the barrier during a 10-min trial. Figure 1C shows that failure to cross the barrier increases with temperature. This behavioral function has a half-activation temperature of ~25°, near the upper limit of fertility, and saturates at temperatures higher than 31°. These results define the

range of temperatures in which heat avoidance occurs in *C. elegans*. For this study, all animals were cultivated at 20° prior to starvation and behavioral assays. It remains to be determined whether the threshold for heat avoidance is fixed or varies with cultivation temperature.

Having identified the temperature range in which avoidance occurs, we developed the noxious heat thermogradient assay (Figure 2), which exposes animals only to temperatures between 29° and 37°. As in the barrier assay, this assay used a cocktail of attractive odorants. At constant temperature, the distribution of animals was skewed toward the attractant cocktail on the right-hand side of the assay plate (Figure 2B). Superimposition of a thermal gradient ranging from 29° to 37° (left to right) induced a pronounced shift in the distribution away from warm temperatures and the attractants, suggesting that heat-induced repulsion can overcome chemical attraction (compare Figure 2B and 2C). We note that heat-induced repulsion was observed with and without the attractant cocktail (Figure 2C).

TRP channel mutants produce modest defects in heat avoidance: Reports diverge regarding the number and the identity of the genes included in the TRP channel family in *C. elegans* (Goodman and Schwarz 2003; Kahn-Kirby and Bargmann 2006). Using a phylogenetic approach targeting the region close to the pore loop (see materials and methods), we revisited this question and identified a total of 24 genes encoding predicted TRP channels (Figure S2). To evaluate the potential contribution of those genes to the heat avoidance behavior in *C. elegans*, we used the thermal barrier assay to test heat avoidance in 18 mutant strains with defects in single TRP channel genes. Most of these alleles are either confirmed or predicted loss-of-function alleles. Of these 18 mutants, only *osm-9(ky10)* had a detectable, but modest defect in heat avoidance (Table 1).

osm-9 is most closely related to the mammalian TRPV subfamily of heat-activated channels (Figure S2), raising the possibility that TRPV homologs could act redundantly to mediate heat avoidance in *C. elegans*. To test this idea, we analyzed strains carrying mutations in multiple genes in the TRPV subfamily. We found that *osm-9 ocr-2* and *ocr-1; ocr-2* double mutants, as well as the *ocr-1; osm-9 ocr-2* triple mutants had more pronounced defects in heat avoidance than *osm-9* single mutants (Figure 3A). When tested in the noxious heat thermogradient assay, the distribution of the double mutant *osm-9 ocr-2* shifted toward higher temperatures, consistent with a partial defect in heat avoidance (Figure 3B). As a simple index to compare distributions across strains, we calculated the fraction of worms that migrated beyond the gradient midpoint of 33°. This index, the fraction >33°, was significantly larger in *osm-9 ocr-2* than in N2 (Figure 3C). These two behavior assays indicate that heat avoidance behavior is largely retained in animals with mutations in several TRPV genes. This suggests either a very high level of functional redundancy or the existence of TRPV channel-independent pathways of heat sensation and avoidance.

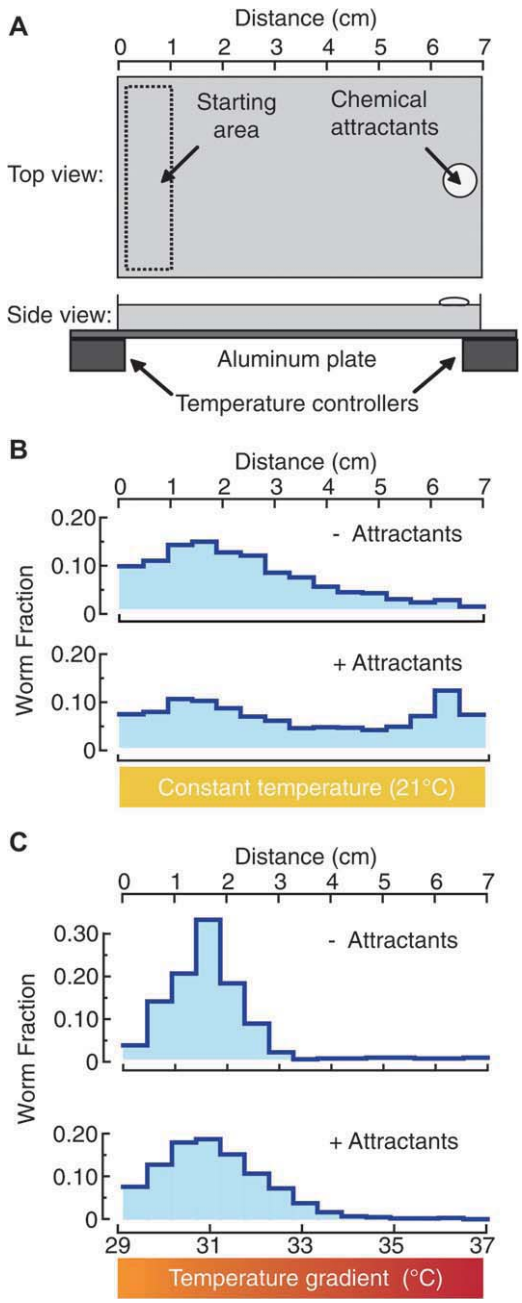

Figure 2.—The *noxious heat thermogradient assay*. (A) Schematic of the noxious heat thermogradient assay. Between 200 and 400 animals are placed on one side of a rectangular Petri dish (starting area) opposite a cocktail of chemical attractants (isoamyl alcohol and 2,3-butanedione). Temperature controllers are used to create either an isothermal environment (T = 21°) or a thermal gradient (29°–37°, 1.15°/cm). (B) Distribution of N2 animals after a 15-min trial at constant temperature (21°) in the absence (top) or presence (bottom) of chemical attractants. Data are the average of at least four assays. (C) Distribution of animals after a 15-min trial on a thermal gradient (29°–37°, 1.15°/cm) in the absence (top) or presence (bottom) of chemical attractants. Data are the average of at least four assays.

The threshold for heat avoidance is higher in CB4856 than N2 animals: To determine how the threshold for

TABLE 1

The effect of TRP channel mutations on noxious heat avoidance

Subfamily	Gene name	Percentage avoiding (mean ± SD)[a]
TRPML	*cup-5*	99 ± 1
TRPA	*trpa-1*	96 ± 1
	trpa-2	93 ± 3
TRPC	*trp-1*	95 ± 3
	trp-2	100 ± 0
TRPN	*trp-4*	98 ± 1
TRPM	*gon-2*	99 ± 1
	gtl-1	100 ± 0
	F56F11.5	92 ± 5
	W03B1.2	95 ± 2
	F13B12.3	99 ± 1
TRPP	*pkd-2*	100 ± 0
	lov-1	97 ± 2
TRPV	*osm-9*	89 ± 2*
	ocr-1	99 ± 0
	ocr-2	94 ± 4
	ocr-3	95 ± 3
	ocr-4	99 ± 9
–	Wild type (N2)	97 ± 1

At least four assays conducted per genotype. One-way ANOVA $F_{(18,135)} = 1.99$, $P = 0.01$. *$P = 0.02$ *vs.* N2 by Dunnet posthoc tests.

[a]Average fraction of animals avoiding the thermal barrier ($T = 32°$), normalized to respective control assays with no heat.

heat avoidance varies among wild isolates of *C. elegans*, we compared noxious heat avoidance in two strains that exhibit a high degree of mutual genetic divergence: Bristol (N2) and Hawaiian (CB4856). In both wild isolates, significantly more animals migrate past the gradient's midpoint temperature of 33° in the presence of the odorant cocktail than in its absence (Figure 4A, left *vs.* right). Under both conditions, the distribution of CB4856 worms was shifted toward higher temperatures (Figure 4A) and the fraction >33° was 5- to 10-fold larger (Figure 4B), indicating that CB4856 tolerates higher temperatures. This difference in performance is not due to differences in attraction to the odorant cocktail, however, since both strains performed similarly in isothermal chemical gradients (Figure S1). Consistent with an increase in the threshold for heat avoidance, the fraction of worms avoiding the barrier in the thermal barrier assay was decreased in CB4856 animals compared to N2 (Figure S3). These results are consistent with the simple model that CB4856 has a higher threshold for heat avoidance, but do not exclude the possibility of synergetic effects of polymorphisms in both chemosensation and heat avoidance.

The polymorphism in heat avoidance threshold is linked to chromosome X: To determine the genetic basis for the difference in heat avoidance between N2 and CB4856 animals, we tested whether any single CB4856 chromosome would be sufficient to increase the temperature threshold. To that purpose, we measured heat avoidance behavior in a set of chromosome substitution strains (CSS) (W. C. Chen and M.-W. Tan, unpublished results). The genome of each of the CSS strains contains five N2 chromosomes and one CB4856 chromosome.

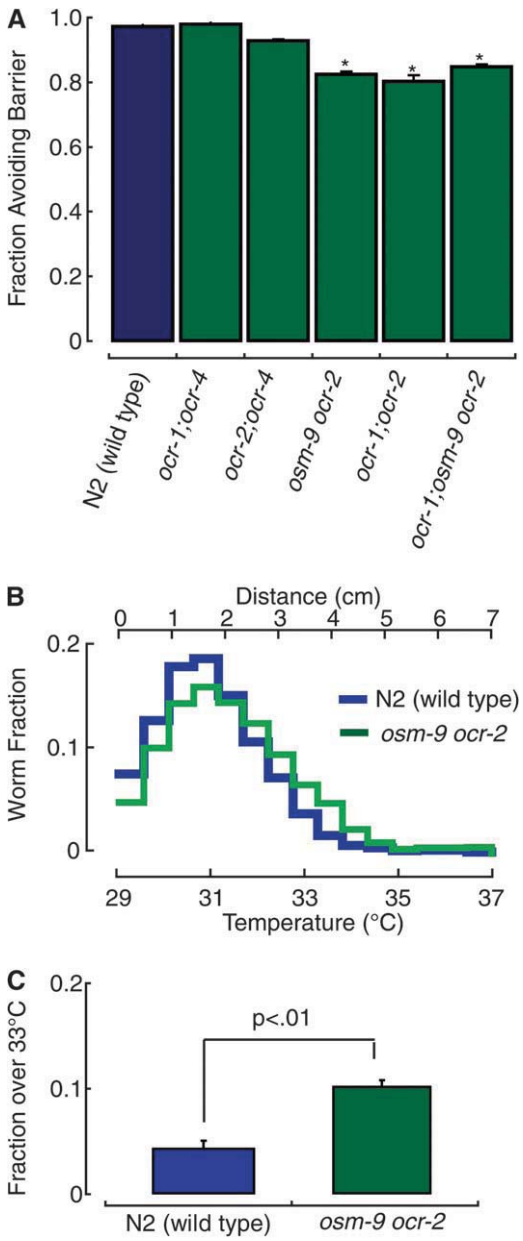

Figure 3.—Mutations in TRPV channel genes cause moderate defects in heat avoidance. (A) Comparison of the performance of wild type (N2) and TRPV mutants in the *thermal barrier assay* ($T_{barrier} = 32°$). The fraction avoiding the barrier was normalized to the corresponding fraction in absence of heat; bars are mean (± SEM) of at least seven assays per genotype. The effect of genotype on heat avoidance was modest, but statistically significant (one-way ANOVA, $F_{(5,104)} = 9.87$, $P < 0.01$. *$P < 0.01$ *vs.* N2 by Dunnet posthoc tests). (B and C) The performance of N2 and *osm-9(ky10) ocr-2(ak47)* double mutants in the *noxious heat thermogradient assay.* (B) Distribution profiles following a 15-min assay in the presence of attractant. (C) The fraction >33° calculated from the distribution profiles reported in B. The difference between N2 and *osm-9(ky10) ocr-2 (ak47)* is statistically significant (Student's *t*-test, $P < 0.01$).

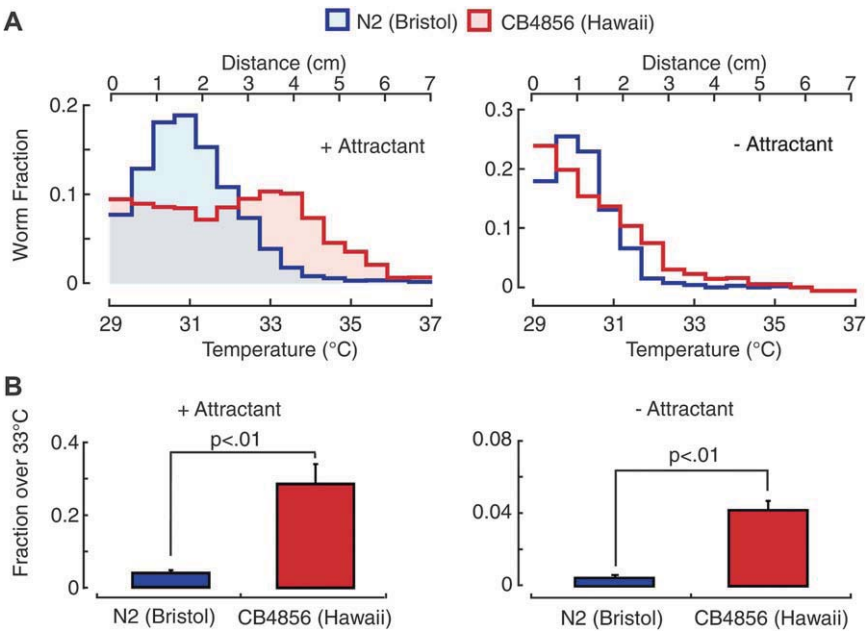

FIGURE 4.—The threshold for heat avoidance is higher in CB4856 than in N2. (A) Distribution profiles following a 15-min assay in the presence (left) and absence (right) of the attractant cocktail. Blue: N2 (Bristol); red: CB4856 (Hawaii). (B) The fraction >33°, calculated from the distribution profiles reported in A. The response of N2 and CB4856 are significantly different (Student's *t*-test, $P < 0.01$) in the presence (left) and absence (right) of the attractant cocktail. For assays conducted in the absence of the attractant cocktail, the data are plotted on an expanded scale since fewer animals of both genotypes migrate beyond the gradient's midpoint of 33° under these conditions.

The response of the CSSI, CSSII, CSSIII, CSSIV, and CSSV strains in the thermogradient assay is similar to N2, but CSSX behaves like CB4856 (Figure 5A). This observation indicates that the X chromosome from the CB4856 strain is sufficient to cause the elevation in temperature threshold. Additionally, we generated a CSSXB strain in which most of the genome is from CB4856, except chromosome X and a small stretch on chromosome I that are from N2. The heat avoidance behavior of this strain was similar to that of N2 (Figure 5A). Thus, genetic variations on chromosome X regulate the threshold for heat avoidance in *C. elegans*.

Next, we used SNP mapping to determine which part of chromosome X is associated with this phenotype (Figure 5B). The data reveal a significant association with the left arm of chromosome X and detailed analysis of recombinants pointed toward a locus located between −8.14 and −4.05 cM (not shown). Consistent with analysis of the chromosome substitution strains (Figure 5A), similar SNP analyses conducted with markers on the autosomes did not detect any other association (Figure S4). We refined this polymorphic locus further by determining the heat avoidance phenotype of QX1155, a strain in which the region between −6.21 and −11.3 cM on the X chromosome of the CB4856 strain has been introgressed into the N2 background (McGrath *et al.* 2009). This strain has a significantly higher temperature threshold than N2 (Figure 5C), although the score was lower than that of CB4856. These results indicate that at least one locus within the region covered by the introgression makes a critical contribution to the temperature threshold for heat avoidance, but do not rule out contributions from additional loci outside this region.

A polymorphism in *npr-1* accounts for the variation in heat avoidance: Polymorphisms in the neuropeptide receptor gene, *npr-1*, affect diverse *C. elegans* behaviors (de Bono and Bargmann 1998; Davies *et al.* 2004; Gloria-Soria and Azevedo 2008). The NPR-1(215V) variant, which is present in N2, is dominant over the NPR-1(215F) variant, which is present in CB4856, regarding the social feeding behavior phenotype (de Bono and Bargmann 1998). The polymorphism in *npr-1* represents a good candidate for explaining the difference in heat avoidance, since the gene is located on chromosome X at −6.66 cM, which is both within our mapped interval and part of the introgressed region in the QX1155 strain (Figure 5C). To determine whether this polymorphism in *npr-1* is responsible for the differential temperature threshold, we compared the behavior of transgenic animals created by McGrath *et al.* (2009) in which an NPR-1(215V) transgene is expressed under the control of *npr-1* promoter in an NPR-1(215F)-containing background (QX1155). The results show that expression of the N2 variant (215V) was sufficient to restore a low threshold, similar to that of N2 worms (Figure 6A). Conversely, transgenic expression of the 215F variant in the same background did not lower the temperature threshold. The difference in heat avoidance is not due to variation in chemosensation, since the two transgenic strains had essentially identical responses to chemical attractants in isothermal conditions (Figure S5). Thus, the N2 variant of NPR-1(215V) confers a low temperature threshold and is dominant over the CB4856 variant of NPR-1(215F), which confers a high temperature threshold.

We evaluated whether the 215V/215F polymorphism was linked to differential responses to noxious heat in two additional wild isolates of *C. elegans* that carry the same polymorphism in the *npr-1* gene (de Bono and Bargmann

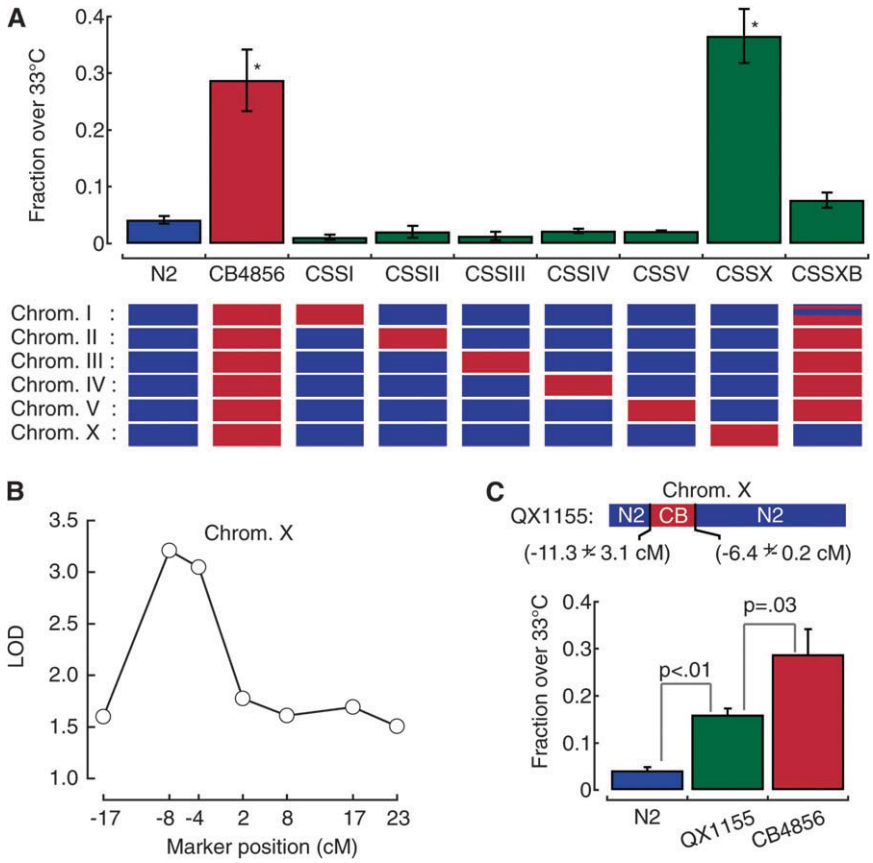

FIGURE 5.—The polymorphism in thermal threshold is linked to chromosome X. (A) Heat avoidance behavior in N2, CB4856, and several chromosome substitution strains. Behavior was evaluated with the *noxious heat thermogradient assay* and reported as the fraction of animals accumulating >33° after 15 min. Bars are the mean (± SEM) of at least six assays. The chromosome of origin (N2 in blue; CB4856 in red) is shown schematically beneath each bar. The effect of genotype on behavior was statistically significant: one-way ANOVA, $F_{(8,123)} = 49.74$, $P < 0.01$. $^*P < 0.001$ *vs.* N2 by Dunnet posthoc tests. (B) LOD scores obtained along chromosome X with a SNP marker mapping approach. (C) Heat avoidance behavior of the QX1155 introgression strain compared to N2 and CB4856. In the QX1155 strain, the indicated portion of the X chromosome from CB4856 origin was introgressed into a N2 background. Bars are the mean (± SEM, $n \geq 8$ assays). The effect of genotype on behavior was statistically significant (one-way ANOVA, $F_{(2,60)} = 34.18$, $P < 0.01$. Indicated P values were obtained by Tukey HSD posthoc tests). All the results derived from noxious heat thermogradient assays.

1998): TR403 NPR-1(215V) and AB3 NPR-1(215F). A strong correlation between genotype and phenotype is evident since the TR403 strain had a low threshold of heat avoidance, similar to N2 (fraction >33° = 0.01 ± 0.01, mean ± SEM, $n = 4$), while the AB3 strain had a higher threshold for heat avoidance, similar to CB4856 (fraction >33° = 0.33 ± 0.04, mean ± SEM, $n = 4$). Collectively, our data show that the NPR-1 215V/215F polymorphism regulates the threshold for heat avoidance.

***npr-1* loss-of-function mutations increase the threshold for heat avoidance:** To further evaluate the role of *npr-1* in determining the temperature threshold of noxious heat avoidance, three loss-of-function mutants of *npr-1* were analyzed. All three mutants, *npr-1(ky13)*, *npr-1(ad609)*, and *npr-1(n1353)* were generated in the N2 background (de Bono and Bargmann 1998). Consistent with the idea that NPR-1(215V) lowers the threshold for heat avoidance, the three *npr-1* loss-of-function mutants had significantly higher thermal thresholds than wild-type N2 worms (Figure 6B).

Loss of the NPR-1 ligand FLP-21 increases the threshold for heat avoidance: We next addressed whether the NPR-1 ligand, FLP-21 (Rogers *et al.* 2003), was involved in establishing the threshold for heat avoidance. To test this idea, we analyzed the thermal avoidance behavior of *flp-21(ok889)*, a strain in which the coding region of the *flp-21* preproprotein gene is deleted. Figure 6C shows that the *flp-21(ok889)* mutant has a significantly increased temperature threshold for heat avoidance, indistinguishable from the *npr-1* loss-of-function mutants. The *flp-21(ok889); npr-1(ad609)* double-mutant behavior was not different from either single mutant, indicating that both genes operate in the same genetic pathway (Figure 6C). Together, our data establish that the FLP-21/NPR-1 neuropeptide pathway functions to maintain a low temperature threshold for heat avoidance.

***npr-1* controls heat avoidance nonredundantly with *osm-9* and *ocr-2*:** The effect of loss of *npr-1* function on social feeding behavior is suppressed by loss-of-function mutations in *osm-9* (de Bono *et al.* 2002). By contrast, the effect of *npr-1* on heat avoidance is not suppressed by *osm-9*: the heat avoidance phenotype of *npr-1(ad609); osm-9(ky10)* double mutants is indistinguishable from that of *npr-1(ad609)* single mutants (not shown). Because *osm-9* mutants have only a mild defect in heat avoidance, however, it was not possible to determine whether or not this mutation has a cumulative effect with the *npr-1* mutation. To learn more about possible interactions between NPR-1– and TRPV-dependent signaling, we compared the phenotype of *osm-9 ocr-2* double mutants with *osm-9 ocr-2; npr-1(ad609)* triple mutants. Interestingly, we found that the heat avoidance defect of the triple mutant was more severe than that of *npr-1*

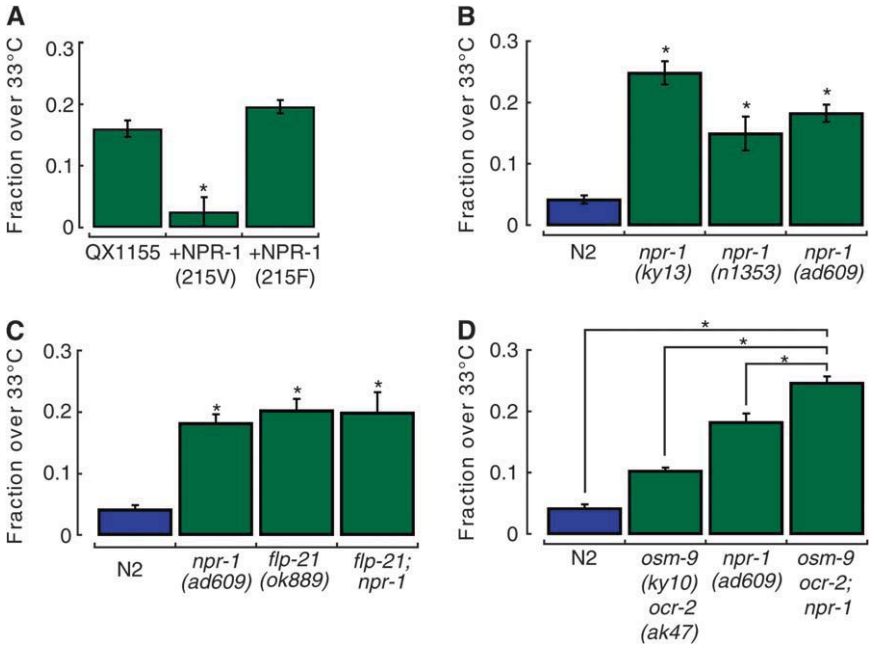

FIGURE 6.—Inactivation of NPR-1 signaling increases the threshold for heat avoidance in both wild type (N2) and *osm-9 ocr-2* double mutants. (A) Heat avoidance in transgenic animals expressing NPR-1 variants in the QX1155 background, which carries the 215F variant of NPR-1. Bars are the average (± SEM, $n \geq 4$). Genotypes significantly altered behavioral scores: one-way ANOVA, $F_{(2,12)} = 13.11$, $P < 0.01$. $^*P < 0.01$ *vs.* QX1155 by Tukey HSD posthoc tests. (B) Heat avoidance of *npr-1* loss-of-function mutants *vs.* N2. Bars are the average (± SEM, $n \geq 7$). Genotypes significantly altered behavioral scores: one-way ANOVA, $F_{(3,73)} = 54.65$, $P < 0.01$. $^*P < 0.01$ *vs.* N2 by Tukey HSD posthoc tests. (C) Heat avoidance of *flp-21* null mutants in N2 and *npr-1(ad609)* background. Bars are the average (± SEM, $n \geq 8$). Genotypes significantly altered behavioral scores: one-way ANOVA, $F_{(3,75)} = 39.31$, $P < 0.01$. $^*P < 0.01$ *vs.* N2 by Tukey HSD posthoc tests; differences among mutants are not significant. (D) Heat avoidance of *osm-9 ocr-2* double mutants, *npr-1*, and the triple mutant *osm-9 ocr-2; npr-1*. Bars are the average (± SEM, $n \geq 7$). Genotypes significantly altered behavioral scores: one-way ANOVA, $F_{(3,73)} = 54.65$, $P < 0.01$. $^*P < 0.01$ by Tukey HSD posthoc tests.

(ad609) single mutants or *osm-9 ocr-2* double mutants (Figure 6D). Thus, *npr-1* and the TRPV genes act synergistically, most likely in parallel genetic pathways.

Animals lacking sensory neurons responsible for thermotaxis, touch sensation, and aerotaxis have normal heat avoidance: The neuronal basis of noxious heat detection and the noxious heat-evoked avoidance response is not known. To gain insight into the neurons required for heat avoidance, we screened strains in which specific candidate neurons had been genetically ablated by transgenic expression of a reconstituted caspase (CHELUR and CHALFIE 2007), the cell-death protein EGL-1 (CHANG *et al.* 2006), or by endogenous expression of a dominant gain-of-function mutation in the *mec-4* gene (DRISCOLL and CHALFIE 1991).

Our first candidate was AFD, a well-characterized sensory neuron involved in thermosensation in the innocuous range of temperature (MORI and OHSHIMA 1995). To determine whether or not AFD is required for noxious heat avoidance, we created transgenic animals expressing a reconstituted caspase under the control of the AFD-specific *gcy-8* promoter (see MATERIALS AND METHODS). Consistent with previously published data using laser ablation (MORI and OHSHIMA 1995; CHUNG *et al.* 2006), genetically ablated AFD animals were partially defective in thermotaxis (Figure 7A), as assessed with behavioral assays on linear thermal gradients (RAMOT *et al.* 2008). In noxious heat avoidance assays, by contrast, AFD ablated animals were indistinguishable from N2 (Figure 7B, Figure S6). Therefore, the thermoreceptor neuron AFD is not required for noxious heat avoidance, which suggests that other sensory neurons are involved.

We continued our investigation by addressing whether the touch receptor neurons (TRNs), which are involved in the avoidance responses induced by gentle body touch, were required for heat avoidance. The six TRNs degenerate in *mec-4(e1611)* mutants (DRISCOLL and CHALFIE 1991), providing a strain that lacks TRNs in adult animals. Our results show that the heat avoidance response in the *mec-4(e1611)* animals is comparable to N2 (Figure 7B), indicating that like AFD the TRNs are not required for the heat avoidance response in N2 worms.

We tested additional candidate sensory neurons among those known to express *npr-1*. The underlying hypothesis was that NPR-1 could function in cells required for noxious heat sensation. NPR-1 is expressed in a large number of worm neurons, including AQR, PQR, and URX sensory neurons involved in aerotaxis (COATES and DE BONO 2002). Expression of the cell death activator EGL-1 under the control of the AQR-, PQR-, and URX-specific *gcy-36* promoter is known to ablate these neurons (CHANG *et al.* 2006; ZIMMER *et al.* 2009). We tested the integrated *Pgcy-36::*EGL-1 transgenic line for defects in noxious heat avoidance and found that animals lacking AQR, PQR, and URX performed like intact, wild-type (N2) animals (Figure 7B). Together, our data indicate that noxious heat avoidance response does not require the AFD thermoreceptor neurons, the touch receptor neurons, or three classes of *npr-1*–expressing sensory neurons, AQR, PQR, and URX.

Cell-specific rescue of *npr-1* mutant implicates the RMG interneurons: To investigate the neural locus of *npr-1* action in heat avoidance, we analyzed transgenic lines in which the *npr-1(ad609)* mutation was rescued by

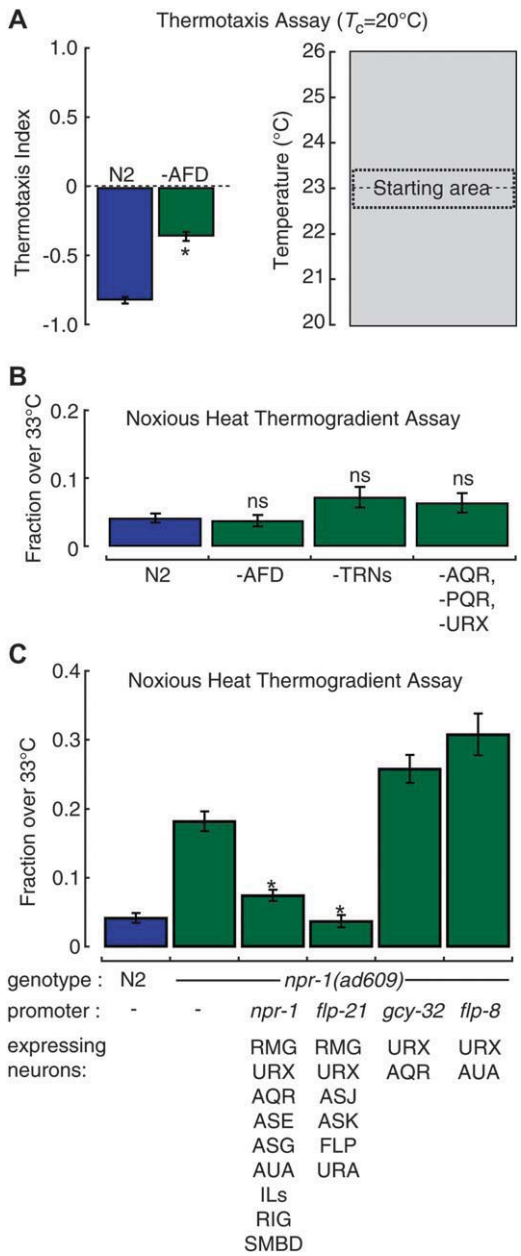

FIGURE 7.—The role of selected sensory neurons and interneurons in heat avoidance. (A) AFD-ablated transgenic animals are partially defective in thermotaxis assayed as shown schematically (right). Well-fed animals were cultivated at 20°, started at 23°, and allowed to migrate for 10 min. Bars are the average (± SEM, $n \geq 21$ assays). *$P < 0.01$ by Student's *t*-test. (B) Performance of transgenic and mutant strains lacking the indicated sensory neurons in the *noxious heat thermogradient assay*. Bars are the mean (± SEM, $n \geq 7$ assays). There was no significant effect of genetic ablation: one-way ANOVA, $F_{(3,64)} = 1.39$, $P = 0.25$. (C) Cell-specific expression of wild-type NPR-1(215V) rescues the defect in heat avoidance in *npr-1(ad609)* null mutants. Bars are the mean fraction >33° (± SEM, $n \geq 8$) in the noxious heat thermogradient assay. The promoters used to drive *npr-1* expression as well as the head neurons where expression is localized (MACOSKO *et al.* 2009) are indicated. Rescue constructs significantly altered behavioral scores: one-way ANOVA, $F_{(5,96)} = 71.62$, $P < 0.01$. * indicates significant decrease compared to *npr-1(ad609)* ($P < 0.01$) by Tukey HSD posthoc tests.

expression of wild-type *npr*-1 cDNA under the control of cell-specific promoters (MACOSKO *et al.* 2009). As expected, expressing wild-type *npr-1* from its own promoter completely rescued heat avoidance (Figure 7C). No rescue was detected using the *gcy-32* or *flp-8* promoters, which drive expression in URX, AQR, and AUA, a subset of *npr-1*–expressing neurons (Figure 7C). Thus, these neurons are probably not involved in *npr-1*–mediated tuning of heat avoidance. By contrast, expressing *npr-1* under the control of the *flp-21* promoter restored heat avoidance to wild type, N2 levels. Collectively, these results implicate the RMG interneurons as the most likely site of action for *npr-1* in the regulation of heat avoidance behavior.

DISCUSSION

Using two quantitative assays of noxious heat avoidance behavior in *C. elegans*, we investigated the genetic and neural basis for this behavior. Our results indicate that both TRPV-dependent and TRPV-independent genetic pathways regulate the threshold for heat avoidance response. From a comparison of N2 and CB4856, which diverge in their response to heat, and from the analysis of several mutants in the N2 background, we showed that the NPR-1/FLP-21 is a TRPV-independent pathway tuning this response. Additionally, we showed that heat avoidance is not dependent on sensory neurons required for thermotaxis (AFD), touch sensation (TRNs), or aerotaxis (AQR, PQR, and URX), but does rely on an intact *npr-1* receptor in the interneuron RMG.

The thermal barrier assay and the noxious heat thermogradient assay: While essential to describe the stereotyped avoidance behavior evoked by heat in *C. elegans*, the single animal methods used in previous studies (WITTENBURG and BAUMEISTER 1999; STEPHENS *et al.* 2008) are labor intensive and measuring the thermal stimulus delivered in each trial is not practical. The two population-based assays developed here provide complementary benefits: they are comparatively high throughput and allow for delivery of measurable thermal stimuli. The use of chemical odorant cocktail in both the thermal barrier and noxious heat thermogradient assays increased the dynamic range of the behavioral readout and helped to reliably identify phenotypic differences. However, care should be taken with the execution of experiments and the interpretation of results. In particular, control experiments in absence of temperature stimuli are needed to assess motility and attraction toward the odorant. Also, it is not possible to exclude complex interaction effects between chemical and thermal stimuli, as the latter will influence evaporation rate, convection, and diffusion coefficients, and, consequently, shape the spatiotemporal pattern of chemical stimulation delivered to worms. There remains, in addition, the possibility that behavioral responses to

the simultaneous presentation of both stimuli engage a more complex circuit than that used to respond to either chemical or thermal stimulation in isolation.

The fraction of worms migrating to temperatures <33° in the noxious heat thermogradient assay provides a simple quantitative measure of the heat avoidance response that is appropriate for this study. This population-based assay is also well suited to forward genetic approaches, in which polyclonal populations can be rapidly screened for heat insensitive individuals (D. A. Glauser and M. B. Goodman, unpublished results). In future studies, it is likely that more information regarding the motor programs engaged during avoidance of noxious heat could be retrieved from a thorough analysis of animal distribution profiles and their kinetics.

***npr-1* affects several behaviors through different pathways:** The NPR-1 215V/215F polymorphism was initially identified in a study addressing a social feeding behavior in which animals form clusters when feeding on bacterial lawn (de Bono and Bargmann 1998). Animals carrying the *npr-1* 215F allele, as well as loss-of-function mutants in *npr-1* and *flp-21* are so-called social feeders, indicating that an inactive FLP-21/NPR-1 pathway promotes social feeding (Rogers *et al.* 2003). The role of NPR-1 in regulating the threshold for noxious heat avoidance has similarities with its role in social feeding behavior, notably the involvement of the FLP-21 ligand (Rogers *et al.* 2003) and of the RMG interneurons (Macosko *et al.* 2009). However, in contrast to the social feeding behavior, the effect of *npr-1* loss-of-function mutation on heat avoidance is not suppressed by *osm-9*.

The 215V/215F polymorphism also influences ethanol-induced paralysis (Davies *et al.* 2004). In the 215F variant, as well as in *npr-1* loss-of-function mutants, acute tolerance to ethanol develops more rapidly. By contrast with social feeding and heat avoidance, the *flp-21* gene does not seem to be involved in this regulation. The *npr-1* and *flp-21* genes are also required for hypoxia-enhanced sensory perception (Pocock and Hobert 2010). By contrast with heat avoidance, this response is restored in *npr-1* mutants by expressing *npr-1* in AQR, PQR, and URX neurons. Thus, NPR-1 signaling modulates social feeding, ethanol tolerance, hypoxia-enhanced sensory perception, and heat avoidance through overlapping, but nonidentical molecular and neural pathways.

Molecules and neurons involved in heat avoidance behavior: Several TRP channels are intrinsically temperature dependent and are considered to be the dominant class of thermosensor molecules responsible for thermal nociception in mammals (Tominaga 2007). However, here we show that loss-of-function mutations in most *C. elegans* TRP channel genes induce little or no defect in heat avoidance. Even when multiple mutations within the TRPV subfamily are combined, defects remain modest. This suggests that noxious heat sensation operates in *C. elegans* through both TRPV-dependent and TRPV-independent pathways. On the basis of our epistasis analysis, we propose that FLP-21/NPR-1 signaling is a TRPV-independent pathway. However, given their biochemical natures, their widespread expression in the *C. elegans* nervous system, and their involvement in several sensory modalities, it is unlikely that *npr-1* and *flp-21* genes encode specialized thermoreceptor molecules. Instead, we propose that FLP-21/NPR-1 neuropeptide signaling links heat sensation to behavioral responses by acting downstream of thermoreceptor neurons, an inference that is consistent with the implication of RMG interneurons as the cellular locus of NPR-1 function.

The thermoreceptor neurons implicated in heat detection and driving heat avoidance response are not yet known. Our results indicate that the AFD neurons, the touch receptor neurons, and the oxygen sensing neurons are not required for the noxious heat avoidance response, at least under the conditions used for our assays. While not ruling out the possibility that they work redundantly with each other or with other sensory neurons, our results indicate that these neurons do not play a major role in noxious heat sensation. Thus, innocuous and noxious temperature sensation rely on distinct neuronal pathways, which is consistent with the previous observation showing that *ttx-1* mutant animals, in which AFD development is impaired, produce intact heat avoidance responses (Wittenburg and Baumeister 1999). Recent Ca^{2+} imaging experiments have shown that the FLP neurons can be activated by a temperature rise from 20° to 35° (Chatzigeorgiou *et al.* 2010). These neurons, which also express *osm-9* (Tobin *et al.* 2002), are therefore likely candidates that may mediate noxious heat avoidance and will deserve further analyses.

While the NPR-1 genetic polymorphism is sufficient to explain the majority of the phenotypic difference between N2 and CB4856, our data also suggest that additional loci might be involved. However, our experimental approach was not designed to track interaction effects from multiple loci. In a recent study, a polymorphism in the *glb-5* gene was shown to modulate oxygen-driven behavior jointly with *npr-1* (McGrath *et al.* 2009). Future studies using similar QTL approaches are likely to provide a more comprehensive view on the genetic interactions that might tune *C. elegans* thermosensory behaviors.

We thank anonymous reviewers for comments; K. Shen for assistance with SNP mapping and generating the AFD-killed strain; C. Bargmann, M. Chalfie, A. Hart, and M. Koelle for the essential and generous gift of many mutant and transgenic strains; M. De Bono and M. Chalfie for plasmids; A. Samuel and D. Profitt for assistance with the LED ring light; and WormBase. Some strains were provided by the Caenorhabditis Genetics Center, which is funded by the National Institutes of Health (NIH) National Center for Research Resources (NCRR). This research was supported by grants from the NIH to M.B.G. (NS061147) and to M.-W.T. (GM66269); the National Science Foundation to M.B.G.

(NSF0725079); a prospective researcher fellowship from the Swiss National Science Foundation to D.A.G (PBGE33-121191); Stanford Faculty of Medicine dean fellowships to D.A.G and B.L.M., respectively; and the Human Frontiers Science Program (B.L.M.).

LITERATURE CITED

Anderson, J. L., L. Albergotti, S. Proulx, C. Peden, R. B. Huey *et al.*, 2007 Thermal preference of *Caenorhabditis elegans*: a null model and empirical tests. J. Exp. Biol. **210:** 3107–3116.

Brenner, S., 1974 The genetics of *Caenorhabditis elegans*. Genetics **77:** 71–94.

Chang, A. J., N. Chronis, D. S. Karow, M. A. Marletta and C. I. Bargmann, 2006 A distributed chemosensory circuit for oxygen preference in *C. elegans*. PLoS Biol. **4:** e274.

Chatzigeorgiou, M., S. Yoo, J. D. Watson, W. H. Lee, W. C. Spencer *et al.*, 2010 Specific roles for DEG/ENaC and TRP channels in touch and thermosensation in *C. elegans* nociceptors. Nat. Neurosci. **13:** 861–868.

Chelur, D. S., and M. Chalfie, 2007 Targeted cell killing by reconstituted caspases. Proc. Natl. Acad. Sci. USA **104:** 2283–2288.

Chi, C. A., D. A. Clark, S. Lee, D. Biron, L. Luo *et al.*, 2007 Temperature and food mediate long-term thermotactic behavioral plasticity by association-independent mechanisms in *C. elegans*. J. Exp. Biol. **210:** 4043–4052.

Chung, S. H., D. A. Clark, C. V. Gabel, E. Mazur and A. D. Samuel, 2006 The role of the AFD neuron in *C. elegans* thermotaxis analyzed using femtosecond laser ablation. BMC Neurosci. **7:** 30.

Coates, J. C., and M. de Bono, 2002 Antagonistic pathways in neurons exposed to body fluid regulate social feeding in *Caenorhabditis elegans*. Nature **419:** 925–929.

Cutter, A. D., 2006 Nucleotide polymorphism and linkage disequilibrium in wild populations of the partial selfer *Caenorhabditis elegans*. Genetics **172:** 171–184.

Davies, A. G., J. C. Bettinger, T. R. Thiele, M. E. Judy and S. L. McIntire, 2004 Natural variation in the npr-1 gene modifies ethanol responses of wild strains of *C. elegans*. Neuron **42:** 731–743.

Davis, M. W., M. Hammarlund, T. Harrach, P. Hullett, S. Olsen *et al.*, 2005 Rapid single nucleotide polymorphism mapping in *C. elegans*. BMC Genomics **6:** 118.

de Bono, M., and C. I. Bargmann, 1998 Natural variation in a neuropeptide Y receptor homolog modifies social behavior and food response in *C. elegans*. Cell **94:** 679–689.

de Bono, M., D. M. Tobin, M. W. Davis, L. Avery and C. I. Bargmann, 2002 Social feeding in *Caenorhabditis elegans* is induced by neurons that detect aversive stimuli. Nature **419:** 899–903.

Diatchenko, L., G. D. Slade, A. G. Nackley, K. Bhalang, A. Sigurdsson *et al.*, 2005 Genetic basis for individual variations in pain perception and the development of a chronic pain condition. Hum. Mol. Genet. **14:** 135–143.

Do, C. B., M. S. Mahabhashyam, M. Brudno and S. Batzoglou, 2005 ProbCons: probabilistic consistency-based multiple sequence alignment. Genome Res. **15:** 330–340.

Doroszuk, A., L. B. Snoek, E. Fradin, J. Riksen and J. Kammenga, 2009 A genome-wide library of CB4856/N2 introgression lines of *Caenorhabditis elegans*. Nucleic Acids Res. **37:** e110.

Drenth, J. P., and S. G. Waxman, 2007 Mutations in sodium-channel gene SCN9A cause a spectrum of human genetic pain disorders. J. Clin. Invest. **117:** 3603–3609.

Driscoll, M., and M. Chalfie, 1991 The *mec-4* gene is a member of a family of *Caenorhabditis elegans* genes that can mutate to induce neuronal degeneration. Nature **349:** 588–593.

Felix, M. A., and C. Braendle, 2010 The natural history of *Caenorhabditis elegans*. Curr. Biol. **20:** R965–R969.

Garrity, P. A., M. B. Goodman, A. D. Samuel and P. Sengupta, 2010 Running hot and cold: behavioral strategies, neural circuits, and the molecular machinery for thermotaxis in *C. elegans* and Drosophila. Genes Dev. **24:** 2365–2382.

Gentry, R. L., 1973 Thermoregulatory behavior of eared seals. Behaviour **46:** 73–93.

Gloria-Soria, A., and R. B. Azevedo, 2008 *npr-1* Regulates foraging and dispersal strategies in *Caenorhabditis elegans*. Curr. Biol. **18:** 1694–1699.

Goodman, M. B., and E. M. Schwarz, 2003 Transducing touch in *Caenorhabditis elegans*. Annu. Rev. Physiol. **65:** 429–452.

Guindon, S., F. Delsuc, J. F. Dufayard and O. Gascuel, 2009 Estimating maximum likelihood phylogenies with PhyML. Methods Mol. Biol. **537:** 113–137.

Hafez, E. S. E., 1964 Behavioral thermoregulation in mammals and birds. (A review). Int. J. Bioclim. Biomet. **7:** 231–240.

Hedgecock, E. M., and R. L. Russell, 1975 Normal and mutant thermotaxis in the nematode *Caenorhabditis elegans*. Proc. Natl. Acad. Sci. USA **72:** 4061–4065.

Huey, R. B., 1974 Behavioral thermoregulation in lizards: importance of associated costs. Science **184:** 1001–1003.

Indo, Y., 2001 Molecular basis of congenital insensitivity to pain with anhidrosis (CIPA): mutations and polymorphisms in TRKA (NTRK1) gene encoding the receptor tyrosine kinase for nerve growth factor. Hum. Mutat. **18:** 462–471.

Kahn-Kirby, A. H., and C. I. Bargmann, 2006 TRP channels in *C. elegans*. Annu. Rev. Physiol. **68:** 719–736.

Kammenga, J. E., P. C. Phillips, M. de Bono and A. Doroszuk, 2008 Beyond induced mutants: using worms to study natural variation in genetic pathways. Trends Genet. **24:** 178–185.

Klassen, M. P., and K. Shen, 2007 Wnt signaling positions neuromuscular connectivity by inhibiting synapse formation in *C. elegans*. Cell **130:** 704–716.

Kremeyer, B., F. Lopera, J. J. Cox, A. Momin, F. Rugiero *et al.*, 2010 A gain-of-function mutation in TRPA1 causes familial episodic pain syndrome. Neuron **66:** 671–680.

Le, S. Q., and O. Gascuel, 2008 An improved general amino acid replacement matrix. Mol. Biol. Evol. **25:** 1307–1320.

Loria, P. M., J. Hodgkin and O. Hobert, 2004 A conserved postsynaptic transmembrane protein affecting neuromuscular signaling in *Caenorhabditis elegans*. J. Neurosci. **24:** 2191–2201.

Macosko, E. Z., N. Pokala, E. H. Feinberg, S. H. Chalasani, R. A. Butcher *et al.*, 2009 A hub-and-spoke circuit drives pheromone attraction and social behaviour in *C. elegans*. Nature **458:** 1171–1175.

McGrath, P. T., M. V. Rockman, M. Zimmer, H. Jang, E. Z. Macosko *et al.*, 2009 Quantitative mapping of a digenic behavioral trait implicates globin variation in *C. elegans* sensory behaviors. Neuron **61:** 692–699.

Mori, I., and Y. Ohshima, 1995 Neural regulation of thermotaxis in Caenorhabditis elegans. Nature **376:** 344–348.

Myers, B. R., Y. M. Sigal and D. Julius, 2009 Evolution of thermal response properties in a cold-activated TRP channel. PLoS One **4:** e5741.

Pocock, R., and O. Hobert, 2010 Hypoxia activates a latent circuit for processing gustatory information in *C. elegans*. Nat. Neurosci. **13:** 610–614.

Ramot, D., B. L. MacInnis, H. C. Lee and M. B. Goodman, 2008 Thermotaxis is a robust mechanism for thermoregulation in *Caenorhabditis elegans* nematodes. J. Neurosci. **28:** 12546–12557.

Reimann, F., J. J. Cox, I. Belfer, L. Diatchenko, D. V. Zaykin *et al.*, 2010 Pain perception is altered by a nucleotide polymorphism in SCN9A. Proc. Natl. Acad. Sci. USA **107:** 5148–5153.

Rockman, M. V., and L. Kruglyak, 2009 Recombinational landscape and population genomics of *Caenorhabditis elegans*. PLoS Genet. **5:** e1000419.

Rogers, C., V. Reale, K. Kim, H. Chatwin, C. Li *et al.*, 2003 Inhibition of *Caenorhabditis elegans* social feeding by FMRFamide-related peptide activation of NPR-1. Nat. Neurosci. **6:** 1178–1185.

Seebacher, F., 1999 Behavioural postures and the rate of body temperature change in wild freshwater crocodiles, *Crocodylus johnstoni*. Physiol. Biochem. Zool. **72:** 57–63.

Seidel, H. S., M. V. Rockman and L. Kruglyak, 2008 Widespread genetic incompatibility in *C. elegans* maintained by balancing selection. Science **319:** 589–594.

Sivasundar, A., and J. Hey, 2003 Population genetics of *Caenorhabditis elegans*: the paradox of low polymorphism in a widespread species. Genetics **163:** 147–157.

Stephens, G. J., B. Johnson-Kerner, W. Bialek and W. S. Ryu, 2008 Dimensionality and dynamics in the behavior of *C. elegans*. PLoS Comput. Biol. **4:** e1000028.

Tobin, D. M., D. M. Madsen, A. Kahn-Kirby, E. L. Peckol, G. Moulder *et al.*, 2002 Combinatorial expression of TRPV channel proteins defines their sensory functions and subcellular localization in *C. elegans* neurons. Neuron **35:** 307–318.

Tominaga, M., 2007 Nociception and TRP channels. *Handb Exp Pharmacol* **179:** 489–505.

Wicks, S. R., R. T. Yeh, W. R. Gish, R. H. Waterston and R. H. Plasterk, 2001 Rapid gene mapping in *Caenorhabditis elegans* using a high density polymorphism map. Nat. Genet. **28:** 160–164.

Wittenburg, N., and R. Baumeister, 1999 Thermal avoidance in *Caenorhabditis elegans*: an approach to the study of nociception. Proc. Natl. Acad. Sci. USA **96:** 10477–10482.

Zimmer, M., J. M. Gray, N. Pokala, A. J. Chang, D. S. Karow *et al.*, 2009 Neurons detect increases and decreases in oxygen levels using distinct guanylate cyclases. Neuron **61:** 865–879.

Communicating editor: O. Hobert

GENETICS

Supporting Information
http://www.genetics.org/cgi/content/full/genetics.111.127100/DC1

Heat Avoidance Is Regulated by Transient Receptor Potential (TRP) Channels and a Neuropeptide Signaling Pathway in *Caenorhabditis elegans*

Dominique A. Glauser, Will C. Chen, Rebecca Agin, Bronwyn L. MacInnis, Andrew B. Hellman, Paul A. Garrity, Man-Wah Tan and Miriam B. Goodman

DOI: 10.1534/genetics.111.127100

FILE S1

Movie of the avoidance behavior in the *noxious heat barrier assay*

File S1 is available for download as a compressed (.zip) file at http://www.genetics.org/cgi/content/full/genetics.111.127100/DC1.

The movie is accelerated 12 times. It shows the behavior of a worm population in a barrier assay setup during three phases. In the first phase, the heat barrier is activated (heat on) and worm are left crawling in absence of attractant. In the second phase, heat is still on and attractant is added on the other side of the barrier. In both phases, worms are strongly repelled by the heat barrier. (The metal tube appears as a vertical line in the middle of the field of view). In the third phase, heat is turned off (heat off) and worms start crawling under the metal tube. Note that for the purpose of this movie, the setup was slightly modified compared to the one described in the MATERIAL AND METHODS section: (i) the assay geometry was changed, (ii) the lid was not closed, and (iii) the attractant mix was dropped directly on the agar surface instead of into a well. However, we observed identical behaviors in the regular assay format.

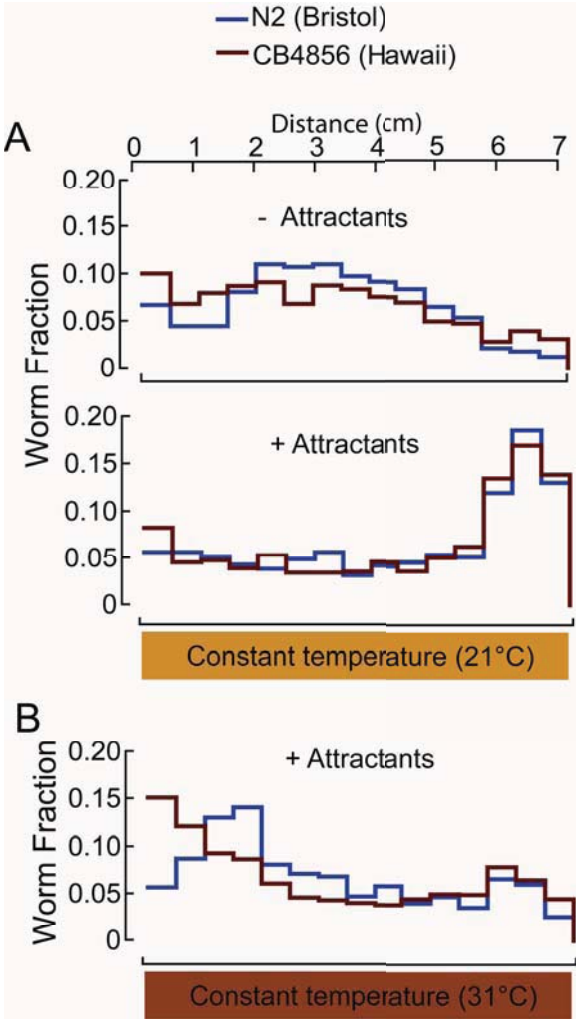

FIGURE S1.—Comparison of CB4856 and N2 in isothermal controls for the *noxious heat thermogradient assay*. The distribution of N2 (blue) and CB4856 (maroon) animals at constant temperature in the absence or presence of the attractant cocktail. (A) T = 21°C. (B) T = 31°C. Results are the mean of at least three independent 15-minute assays.

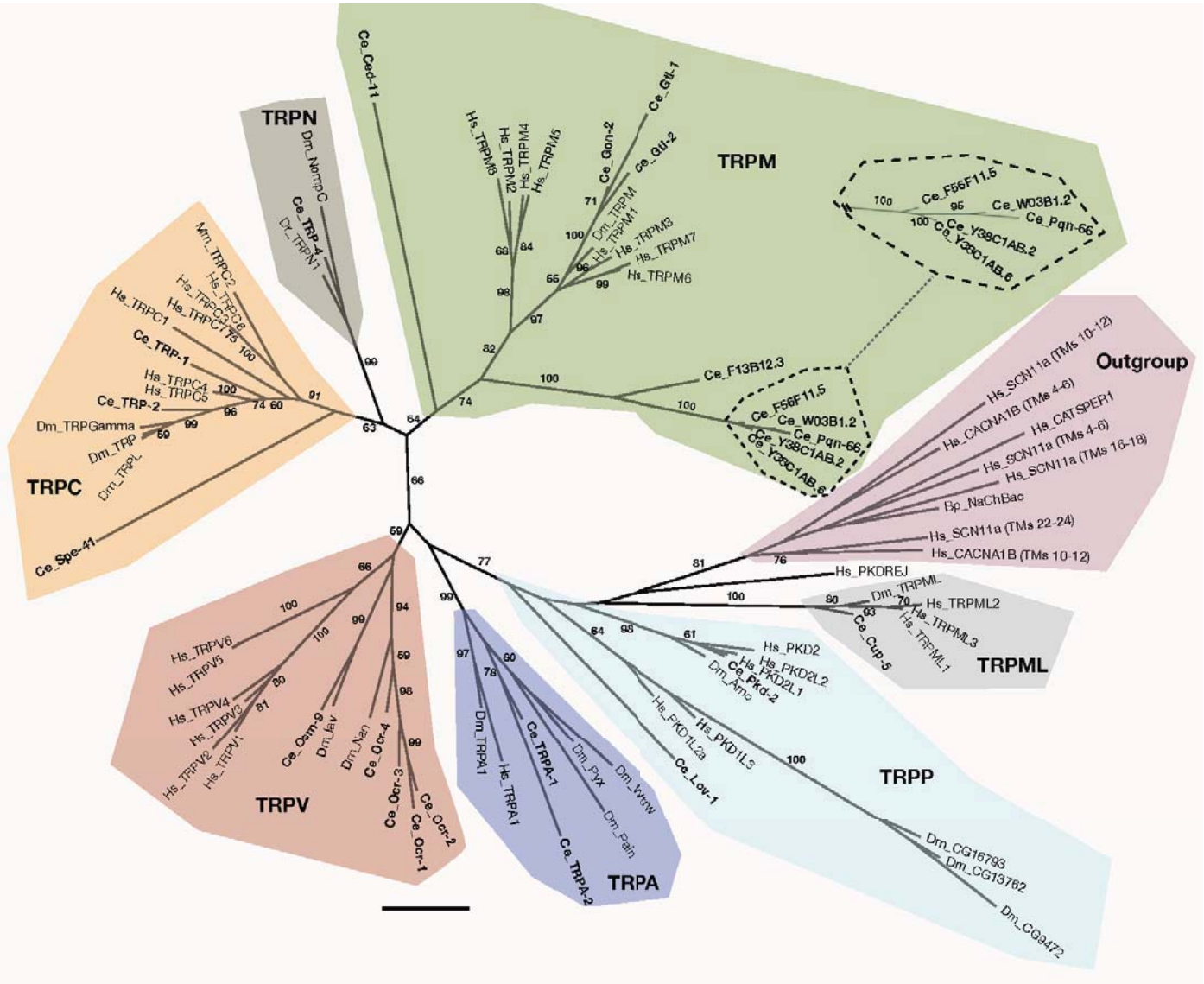

FIGURE S2.—*C. elegans* TRP phylogeny. Phylogeny of *C. elegans* (Ce) transient receptor potential (TRP) channels, with *D. melanogaster* (Dm) and vertebrate TRPs for comparison. Inset shows five closely related *C. elegans* TRPMs. Tree was rooted using *Bacillus pseudofirmus* (Bp) NaChBac and *H. sapiens* (Hs) CACNA1B (N-type voltage-gated calcium channel), SCN11A (voltage-gated sodium channel), and CATSPER1. Vertebrate TRPs are *H. sapiens* (Hs), except for TRPC2 (*M. musculus*, Mm) and TRPN1 (*D. rerio*, Dr). (Hs TRPC2 is a pseudo gene and there is no mammalian ortholog of TRPN1.) CACNA1B and SCN11A contain 24 transmembrane or TM domains; only the TMs indicated were used. Internal branches are labeled with bootstrap percentages. Branches with bootstrap percentages below 55% are unlabeled. Scale bar is 0.8 substitutions per site for main phylogeny, 0.3 for inset.

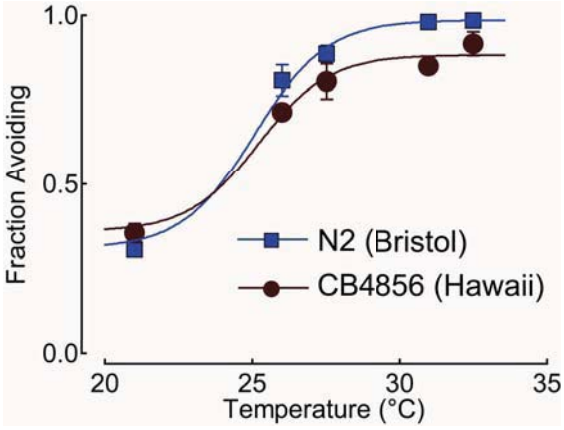

FIGURE S3.—Comparison of CB4856 and N2 in the *noxious heat barrier assay*. Fraction of worms that avoid the heat barrier *vs.* temperature in N2 (blue) and CB4856 (maroon). Adult animals were scored by counting the fraction of the population remaining to the left of the barrier (fraction avoiding) in a 10-minute assay. $T = 21°C$ is the control situation where the metal tube is not heated. Results are the mean of at least three independent assays; error bars are s.e.m. and are smaller than symbols in some cases.

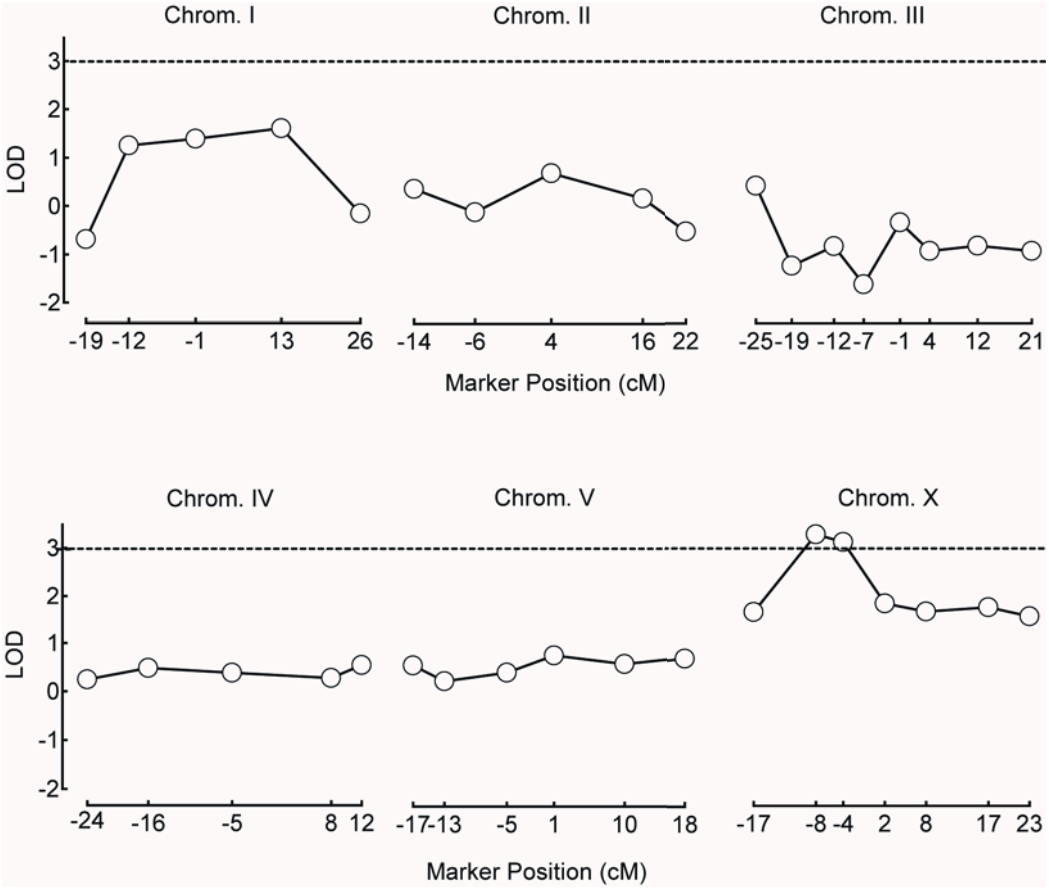

FIGURE S4.—Genome scale SNP mapping analysis. LOD scores derived from SNP marker mapping analyses for each chromosome. See *Materials and Methods* and Figure 5B legend for details. The threshold for significant association was set to 3 (dotted line). Significant linkage was detected only for chromosome X.

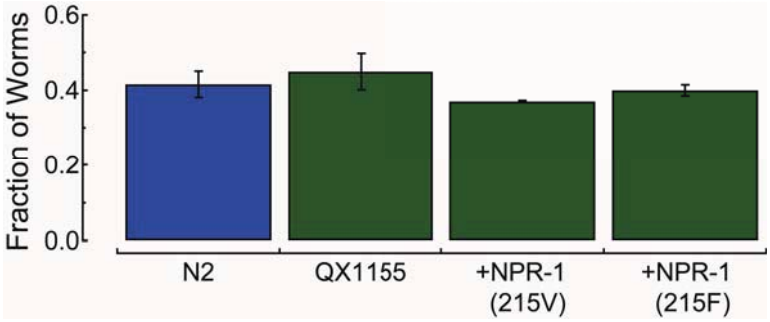

FIGURE S5.—Transgenic animal expressing NPR-1(215V) and NPR-1(215F) behaves like N2 at constant temperature. Worms from indicated genotypes were tested in an isothermal (21°C) environment in the presence of attractants, as depicted in Figure 2B. Scores are presented as fraction of worms that are found to the right of the position corresponding to a temperature of 33°C when temperature gradient is applied. There was no significant effect of genotype: one-way ANOVA, $F_{(3,19)}$=0.22, p = 0.88. Bars are mean ± s.e.m. of at least three independent assays.

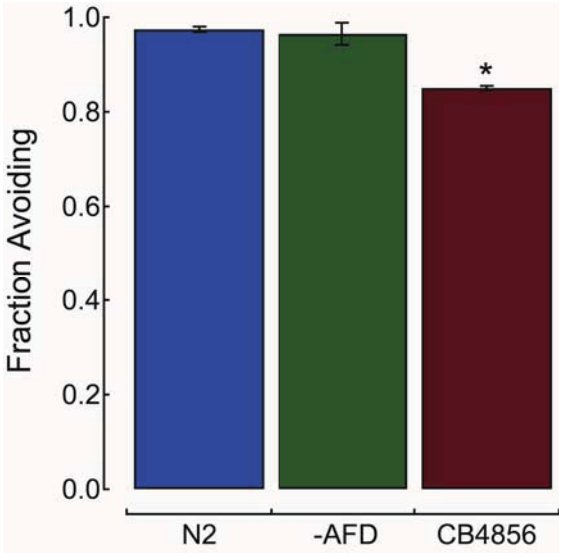

FIGURE S6.—Animals lacking the AFD neurons behave like N2 in *thermal barrier assays*. Fraction of worms with AFD ablated avoiding the barrier in *thermal barrier assays*. A barrier temperature of 31.5°C was used. Bars are the mean (± s.e.m.) of at least four independent assays. The CB4856 score is shown for comparison and was significantly decreased compared to N2. *, $p < 0.01$ by Student's t-test.

TABLE S1

SNP marker survey in CSSXB (*aka* GN360)

Chromosome	Marker Position (cM)	Variant Type
I	-19	CB4856
	-12	N2
	-6	N2
	-1	CB4856
	5	CB4856
	14	CB4856
	26	CB4856
II	-18	CB4856
	-14	CB4856
	-6	CB4856
	1	CB4856
	11	CB4856
	16	CB4856
	22	CB4856
III	-25	CB4856
	-25	CB4856
	-12	CB4856
	-7	CB4856
	4	CB4856
	12	CB4856
	21	CB4856
IV	-24	CB4856
	-16	CB4856
	-5	CB4856
	1	CB4856
	8	CB4856
	14	CB4856
V	-17	CB4856
	-13	CB4856
	-5	CB4856
	1	CB4856
	6	CB4856
	10	CB4856
	13	CB4856
	18	CB4856

	-17	N2
	-8	N2
	-4	N2
X	8	N2
	11	N2
	17	N2
	23	N2